SUPPORTING INFORMATION

FOR THE PAPER: "A THERMODYNAMICALLY CONSISTENT PHASE DIAGRAM OF A TRIMORPHIC PHARMACEUTICAL, L-TYROSINE ETHYL ESTER, BASED ON LIMITED EXPERIMENTAL DATA"

By Béatrice Nicolaï, Maria Barrio, Pol Lloveras, Alain Polian, Jean-Paul Itié, Josep-Lluis Tamarit, Ivo B. Rietveld

UNIT CELL PARAMETERS

Table S1. Fitted unit-cell parameters of forms I, II, and III as a function of pressure and temperature

Form I				
P (MPa)	a (Å)	b (Å)	c (Å)	V (Å^3)
250 K				
0	12.734	16.954	5.274	1139
0	12.728	16.950	5.272	1137
80	12.703	16.963	5.273	1136
190	12.656	16.944	5.248	1126
293 K				
CIF	12.788	16.982	5.279	1146
0	12.762	16.971	5.282	1144
80	12.741	16.975	5.259	1137
270	12.657	16.911	5.204	1114
303 K				
160	12.708	16.978	5.234	1129
323 K				
0	12.837	17.030	5.324	1164
200	12.720	16.959	5.234	1129
0	12.830	17.023	5.331	1164
337 K				
0	12.853	17.026	5.332	1167
200	12.747	16.961	5.252	1136
300	12.674	16.903	5.204	1115
400	12.594	16.800	5.184	1097
60	12.812	17.010	5.314	1158
360 K				
0	12.969	17.042	5.340	1171

Form II				
200 K				
0	12.658	14.624	5.770	1068
100	12.758	14.487	5.695	1053
270	12.737	14.455	5.678	1046
500	12.695	14.403	5.655	1034
850	12.656	14.360	5.628	1023
900	12.648	14.341	5.619	1019
1080	12.629	14.321	5.610	1015
2000	12.567	14.216	5.543	990
2200	12.519	14.167	5.513	978
250 K				
0	12.788	14.670	5.785	1085
110	12.763	14.556	5.760	1070
220	12.720	14.530	5.738	1061
330	12.688	14.504	5.714	1052
500	12.668	14.475	5.687	1043
800	12.648	14.433	5.662	1033
1750	12.580	14.215	5.580	998
293 K				
0	12.754	14.749	5.802	1092
0	12.771	14.739	5.803	1092
0	12.790	14.712	5.805	1092
90	12.745	14.730	5.779	1085
190	12.714	14.689	5.747	1073
300	12.684	14.641	5.714	1061
400	12.649	14.598	5.682	1049
560	12.622	14.554	5.658	1039
830	12.578	14.482	5.612	1022
1200	12.532	14.421	5.580	1008
2400	12.443	14.181	5.472	966
4000	12.420	13.814	5.303	910
Form III				
250 K				
330	12.601	16.015	5.172	1044
600	12.574	16.115	5.147	1043
1000	12.544	16.079	5.131	1035
2100	12.721	15.630	4.978	990
3300	12.530	15.371	4.911	946
4600	12.380	15.147	4.841	908
293 K				
450	12.642	16.005	5.162	1044
800	12.602	15.971	5.122	1031
1600	12.537	15.866	5.074	1009
2100	12.469	15.757	5.033	989
303 K				
440	12.677	16.110	5.236	1069
323 K				
580	12.649	16.060	5.207	1058

720	12.641	16.034	5.184	1051
960	12.607	15.972	5.143	1035
1500	12.538	15.846	5.074	1008
2200	12477	15.721	5.018	984
2500	12.451	15.671	4.997	975
2900	12.411	15.607	4.972	963
3900	12.309	15.442	4.907	933
337 K				
400	12.672	16.116	5.261	1074
500	12.660	16.078	5.225	1064
600	12.638	16.033	5.193	1052
750	12.613	15.999	5.164	1042
4380	12.170	15.281	4.866	905

RAMAN DATA

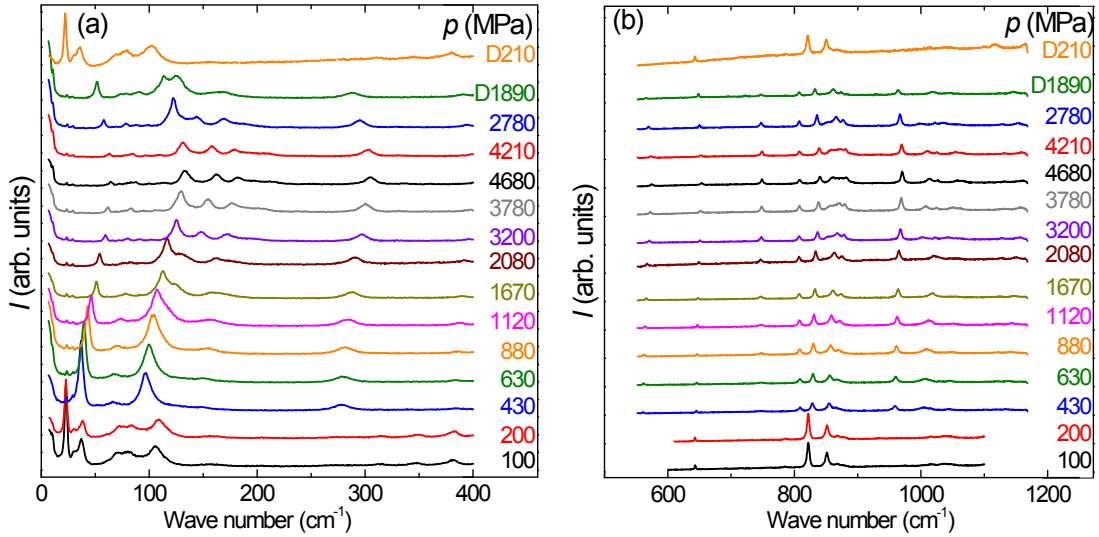

Figure S1. Raman data of form I from 0 to 1200 cm^{-1} at 293 K under pressure. Form I changes into form III between 0.2 and 0.43 GPa. Once returned to 0.21 GPa from 1.89 GPa form I is recovered (D: decompression).

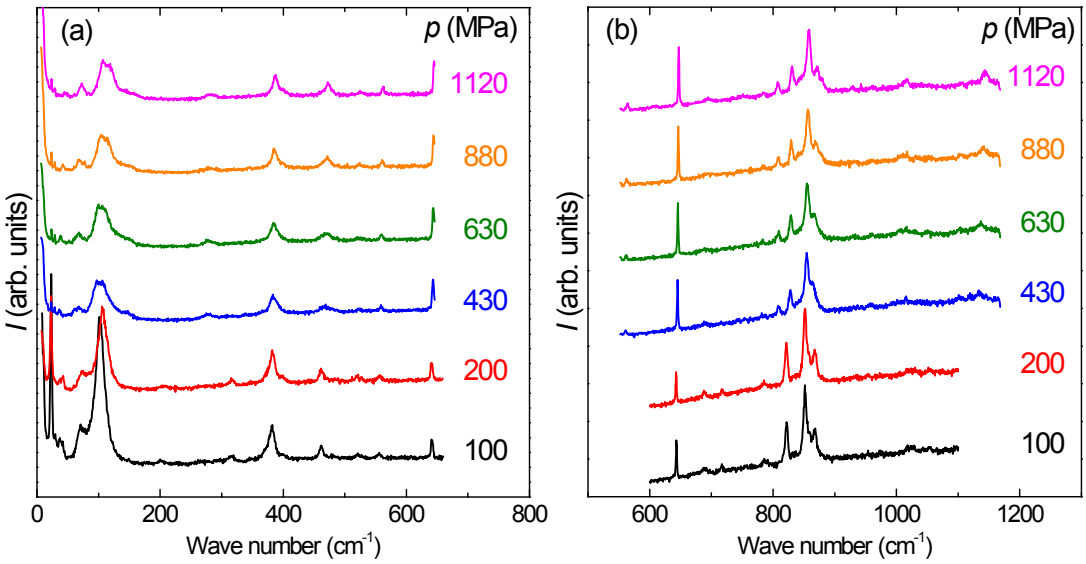

Figure S2. Raman data of form II from 0 to 1200 cm^{-1} at 293 K under pressure. Form II remains unchanged.

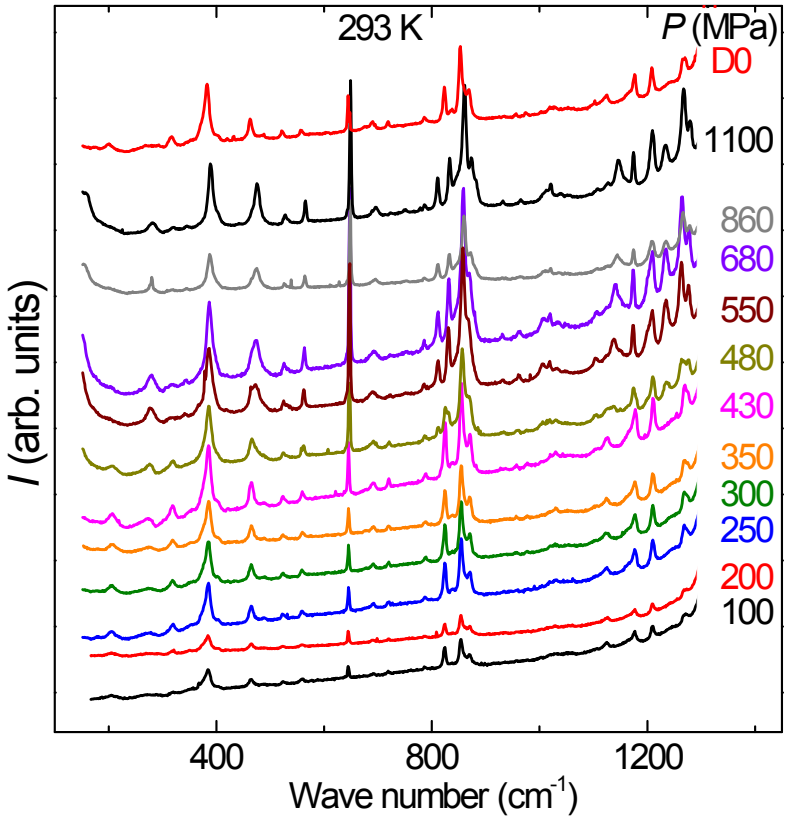

Figure S3. Raman data from 200 to 1300 cm^{-1} at 293 K under pressure. Form I changes into form III between 0.43 and 0.48 GPa (see peak at 800 cm^{-1}), D: decompression.

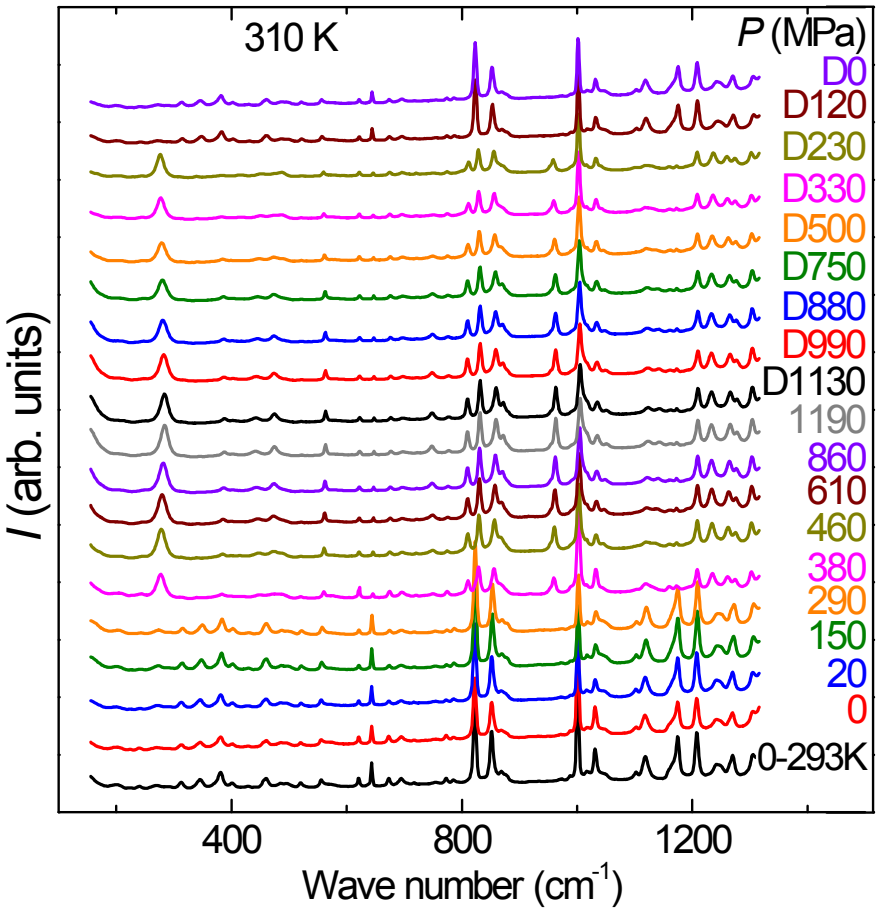

Figure S4. Raman data from 200 to 1300 cm^{-1} at 310 K under pressure. Form I changes into form III between 0.29 and 0.38 GPa (see peaks at 800 and 950 cm^{-1}). Releasing the pressure form I is recovered between 0.23 and 0.12 GPa, D: decompression.

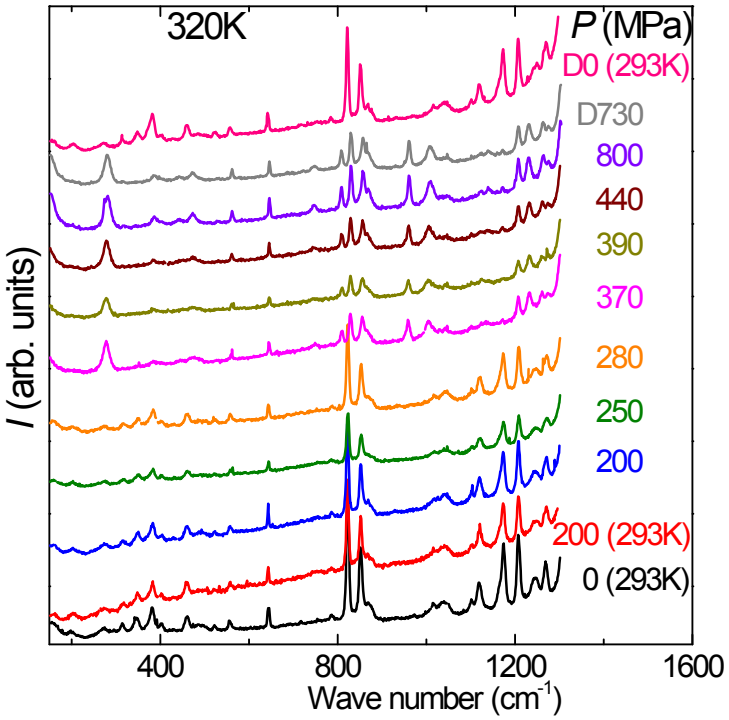

Figure S5. Raman data from 200 to 1300 cm^{-1} at 320 K under pressure. Form I changes into form III between 0.28 and 0.37 GPa (see peaks at 800 and 950 cm^{-1}), D: decompression.

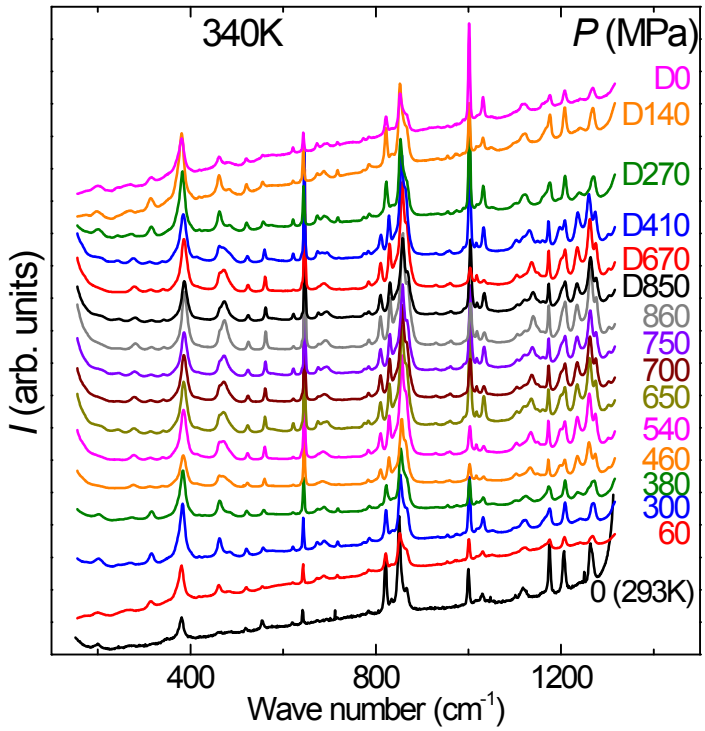

Figure S6. Raman data from 200 to 1300 cm^{-1} at 340 K under pressure. Form I changes into form III between 0.38 and 0.46 GPa (see peak at 800 cm^{-1}) and releasing the pressure form III changes back into form I between 0.41 and 0.27 GPa, D: decompression.

Table S2. Pressures and temperatures at which a different polymorph appears going up in pressure (form III) and going down in pressure (form I) in the diamond anvil cell (Synchrotron and Raman experiments)

T	P I	P III	Source
250	190	300	Synchrotron
293	200	430	Raman
293		480	Raman
293	270	450	Synchrotron
303	160	440	Synchrotron
310	120	380	Raman
320		370	Raman
323	350	580	Synchrotron
337	400	500	Synchrotron
340	410	460	Raman

Table S3. Observed Raman wavenumbers (cm^{-1}) compared with experimental absorption wavenumbers (cm^{-1}) in infrared[a] for L -tyrosine ethyl ester (L-TEE) polymorphs I and II, L –tyrosine methyl ester (L-TME), L –tyrosine propyl ester (L-TPE), and L –tyrosine butyl ester (L-TBE)[b]

	L-TME	L -TEE I		L -TEE II		L -TPE	L -TBE
	IR	IR	Raman	IR	Raman	IR	IR
				3348 sh	3350		
O-H stretch (alcohol)	3353 S	3327 S	3340	3326 S		3344 S	3336 S
				3298 sh	3300		
N-H stretch	3299 m	3269 m	3270	3267 m		3291 m	3287 m
		3160 w		3159 w		3191 vw	3191 w
			3060		3070		
C-H stretch (aromatic)	3012 w		3030	3020 w		2972 w	
C-H stretch	2957 w	2994 w	2960	2940 w	2950	2954 w	2955 S
	2932 w	2945 w	2930	2904 vw	2930		2927 m
	2895 vw	2904 w				2909 w	2904 m
					2880	2851 vw	2869 m
				2792 w			
	2810 vw					2801 vw	2797 w
overtones	2757 vw			2748 w		2761 vw	2743 w
and	2676 w	2676 w		2680 w		2685 m	2676 m
combinations	2586 w	2498 w		2591 w		2589 m	2589 m
				2517 w		2515 m	2515 m
				2345 w		2363 m	
overtones	1893 w						
	1837 w	1881 w		1879 w			1888 w
C=O stretch							

(ester)	1740 vS	1727 vS	1730	1731 vS	1740	1721 vS	1720 vS
	1703 w						
C=C stretch (aromatic)							
	1669 sh					1640 vw	1636 w
N-H bend	1611 m		1615		1615	1614 S	1611 S
C-C stretch (aromatic)	1595 S	1598 S		1592 S	1595	1597 S	1593 S
		1584 S					
C-H bending	1513 S	1514 S		1514 S		1516 vS	1514 vS
O-H bending	1479 S	1454 S	1450	1458 S	1455	1462 S	1459 vS
	1442 S	1439sh		1444sh	1445	1444 sh	
	1435 S	1419 m	1420	1419 w		1396 S	1387 S
	1395 sh						
C-H rock	1379 m	1382 m		1382 m		1379 m	1338 S
	1352 m			1365 w	1350	1347 m	
						1337 m	
	1314 vw	1311 w		1312 m		1298 w	
	1302 m			1298 m	1300		1296 m
C-O stretch (alcohol)			1265		1270		
	1256 vS	1243 vS		1251 vS	1250	1260 vS	1255 vS
	1220 S	1209 m		1220 S		1189 vS	1190 vS
C-O stretch (ester)	1195 S		1205		1205		
	1170 vS	1172 vS	1175	1170 vS	1172	1173 vS	1171 vS
C-O stretch (ester)	1144 vS			1142 m	1145	1143 S	1145 S
	1113 m	1115 m	1120	1115 m			1124 m

C-N stretch	1102 S	1100 m	1100	1100 m	1100	1095 S	1094 S
		1058 S		1061 m		1055 sh	1055 m
	1017 vS	1028 vS		1023 vS		1032 vS	1035 vS
	988 S			972 m		1010sh	1003 vw
	957 m	954 w		954 w		959 m	952 w
	950 m					933 m	932 m
N-H wag	907 m	920 m		907 m		910 vw	
	872 m	865 m		865 m		888 m	878 m
				846 S	855	848 m	867 m
	836 vS	818 vS		815 vS	825	818 vS	820 vS
C-H bend (aromatic)	794 m	780 m		782 m	785	780 S	778 S
		752 m		753 m		748 S	749 m
C-H rock	732 m			731 m			737 m
	719 m	715 w	715	715 w		713 vw	713 vw
		684 m		684 vw		682 m	679 m
	646 w			671 vw			
	636 m	640 m	645	640 m	645	640 m	640 m
				621 sh			
	572 S	558 m	560	572 m			
			520				
			375				
					320		
			100		130		
					95		
			80				

			35 20		60 35 22		

[a] Obtained by FTIR, Perkin Elmer Septum spectrometer 1000

[b] S: strong, vS: very strong, m: medium, w: weak, vw: very weak, sh: shoulder

Wavenumbers lowered by hydrogen bonding

In L-TEE polymorph I, the O-H stretch wavenumber is lower than normal, because of the infinite chain of strong hydrogen bonds, which is consistent with the isobaric thermal expansion tensors published previously.[1-2]

In L–TEE polymorph I, the C=O stretch wavenumber is lower than normal, because the hydrogen bonding between CH_3 and O=C is stronger in polymorph I than in polymorph II (in form II C=O forms a bifurcated hydrogen bond with the CH_3 et CH_2 groups)

The three C-O bonds in each molecule give rise to three different C-O stretch wavenumbers. One of those remains remarkably constant around 1170 cm^{-1}, whereas the others vary much more. The higher wavenumber is most likely the alcohol, whose value depends on hydrogen bonds of different strengths.

UNIT-CELL VOLUMES

Expressions for the unit-cell volumes ($Å^3$) as a function of pressure (MPa) and temperature (K):

Form I (valid for P = 0 – 400 MPa)

337 K: $V_I = 1168.4(1.4) - 0.176(6)\ P$ $R^2 = 0.997$ (SI.1)

293 K: $V_I = 1145.5(9) - 0.116(6)\ P$ $R^2 = 0.994$ (SI.2)

Form II (valid for P = 0 – 850 MPa)

293 K: $V_{II} = 1092.8(8) - 0.120(6)\ P + 4.3(6)\times10^{-5}\ P^2$ $R^2 = 0.998$ (SI.3)

250 K: $V_{II} = 1083.0(1.6) - 0.103(9)\ P + 3.7(9)\times10^{-5}\ P^2$ $R^2 = 0.996$ (SI.4)

200 K: $V_{II} = 1067.6(1.4) - 0.088(8)\,P + 4.0(8)\times10^{-5}\,P^2$ $R^2 = 0.996$ (SI.5)

Form II (800 – 4000 MPa)

All T: $V_{II} = 1053(3) - 0.0349(13)\,P$ $R^2 = 0.987$ (SI.6)

Form III (valid for P = 400 – 1500 MPa)

303 – 337 K: $V_{III} = 1104(8) - 0.091(16)\,P + 1.9(8)\times10^{-5}\,P^2$ $R^2 = 0.984$ (SI.7)

Form III (T = 250, 293 K: valid for all P and T = 303, 323, 337 K: valid for P = 1500 – 4500 MPa)

All T: $V_{III} = 1061(2) - 0.0339(7)\,P$ $R^2 = 0.993$ (SI.8)

TWO-PHASE EQUILIBRIA AND TRIPLE POINTS

Topological calculations of the two-phase equilibria and triple points discussed in the text

I-II: $P = -224.6 + 0.7339\,T$ (SI.9), published in a previous paper.[2]

With triple point (eqs. SI.9 and SI.13):

I-II-V: 306 K, 0.047 Pa

I-L: $P = -3375 + 8.96\,T$ (SI.10), obtained through a linear fit of the melting data of form I under pressure.

With triple point (eqs. SI.10 and SI.12):

I-L-V: 376 K, 57 Pa

The triple point I-II-L, the intersection of SI.9 and SI.10, is:

$(0.7339 - 8.96)/(-3375 + 224.6) = T = 383$ K, leading to 57 MPa with eq. SI.10.

I-II-L: 383 K, 57 MPa

From a previous paper,[2] the following expressions for the vapor pressures of the liquid phase, form I, and form II can be obtained in the form of the Clausius-Clapeyron equation:

$\ln(P) = -\Delta H/(RT) + B$ (SI.11),
with R the gas constant (8.3145 J mol^{-1} K^{-1}) and P in Pa.

L-V: $\ln(P) = -64.69 \times 10^3$ J mol^{-1} $/(RT) + 24.72$ (SI.12)[2]

I-V: $\ln(P) = -96.54 \times 10^3$ J mol^{-1} $/(RT) + 34.89$ (SI.13)[2]

II-V: $\ln(P) = -98.28 \times 10^3$ J mol^{-1} $/(RT) + 35.58$ (SI.14)[2]

Using triple point III-L-V below, the vapor pressure of form III can be given as

III-V: $\ln(P) = -102.98 \times 10^3$ J mol^{-1} $/(RT) + 38.22$ (SI.15)[2]

The triple point II-L-V is equivalent to the melting point of form II under ordinary conditions and can be found through the intersection of the equilibrium lines L-V and II-V.

Thus $T = (-64.69 + 98.28)/(R(35.58 - 24.72))$ leads to a melting point of 372 K at a pressure of 44.7 Pa (triple point II-L-V).

II-L-V: 372 K, 44.7 Pa

The two triple points I-II-L (383 K, 57 MPa) and II-L-V (372 K, 44.7 Pa) lead to the expression for II-L

II-L: $P = -1891 + 5.08\ T$ (SI.16)

The expression for the two-phase equilibrium I-III was obtained by synchrotron X-ray diffraction[3] and improved with Raman data resulting in:

I-III: $P = -439.3 + 2.483\ T$ (SI.17)

With the equation for I-II (eq. SI.9), one finds the triple point

I-II-III: 123 K, −134 MPa

Setting P = 0, one finds the triple point

I-III-V: 177 K, 0 Pa

The pressure can be verified with eq. SI.13 leading to 4.5×10^{-8} Pa.

With the I-II-III triple point and the Clapeyron equation, the II-III equilibrium can be calculated. The Clapeyron equation is:

$$\mathrm{d}P/\mathrm{d}T = \Delta S/\Delta V = \Delta H/(T\Delta V) \qquad \text{(SI.18)}$$

Thus the entropy and volume difference for the II-III transition are needed.

$\Delta_{\mathrm{II}\to\mathrm{I}}h$ = 8.355 J g^{-1} at 306 K; $\Delta_{\mathrm{II}\to\mathrm{I}}s = \Delta_{\mathrm{II}\to\mathrm{I}}h/T$ = 0.0273 J g^{-1} K^{-1} for form II turning into form I.[2] For the I-III transition, at 300 K, the pressure of the equilibrium equals 306 MPa using eq. SI.17. With SI.2 and SI.8, 306 MPa leads to V_{I} = 1110 Å^3 and V_{III} = 1050 Å^3, thus $\Delta_{\mathrm{III}\to\mathrm{I}}V$ = +59.9 Å^3 and with M_{w} = 209.24 g mol^{-1} $\Delta_{\mathrm{III}\to\mathrm{I}}v$ =0.0431 cm^{3}g^{-1}. The slope of I-III is 2.483 MPa K^{-1} (eq. SI.17) multiplied by the change in volume leads to the entropy of transition: $\Delta_{\mathrm{III}\to\mathrm{I}}s$ = 2.483 × 0.0431 = 0.1069 J g^{-1} K^{-1}. III → I → II is equivalent to III → II: the entropy of transition $\Delta_{\mathrm{III}\to\mathrm{II}}s = \Delta_{\mathrm{III}\to\mathrm{I}}s + \Delta_{\mathrm{I}\to\mathrm{II}}s$ = 0.1069 − 0.0273 = 0.0796 J g^{-1} K^{-1}.

The volume difference can be estimated from the volumes of forms II and III at high pressure, 1000 MPa, equations SI.6 and SI.8:

V_{II} = 1053 − 0.0349 ×1000 MPa = 1018.23 Å^3

V_{III} = 1061 − 0.0339 ×1000 MPa = 1026.68 Å^3

$\Delta_{\mathrm{III}\to\mathrm{II}}V$ = 1018.23 − 1026.68 = −8.45 Å^3 = −0.00608 cm^3 g^{-1}

The slope $\mathrm{d}P/\mathrm{d}T$ = 0.0796/−0.00608 = −13.1 MPa K^{-1}

With triple point I-II-III:

II-III: P = 1474 −13.1 T (SI.19)

At P = 0 with II-III (eq SI.19)

II-III-V: 112 K, 0 Pa

With II-III and II-L (eqs. SI.19 and SI.16)

II-III-L: 185 K, −950 MPa

With I-III and I-L (eqs. SI.17 and SI.10)

I-III-L: 453 K, 687 MPa

With triple point II-III-L and I-III-L, the equilibrium line III-L is obtained:

III-L: P = −2078 + 6.1 T (SI.20)

With P = 0 III-L (eq. SI.20) leads to triple point III-L-V temperature 341 K

With the L-V equilibrium (eq. SI.12), the vapor pressure can be calculated:

III-L-V: 341 K, 6.6 Pa

BIRCH-MURNAGHAN FITS OF THE *P*(*V*) DATA

Birch-Murnaghan equation:

$$P = 3K_{0T} f_E \left(1+2f_E\right)^{5/2} \left(1+\tfrac{3}{2}\left(K'_{0T}-4\right)f_E + \tfrac{3}{2}\left(K_{0T}K''_{0T} + \left(K'_{0T}-4\right)\left(K'_{0T}-3\right) + \tfrac{35}{9}\right)f_E^2\right)$$

$$\text{with } f_E = \left[\left(V_{0T}/V\right)^{2/3} - 1\right]\Big/2 \qquad \text{(SI. 21)}$$

P is the pressure, V is the unit-cell volume related to pressure P, V_{0T} is the unit-cell volume at a given temperature at zero pressure, K_{0T} is the bulk modulus for a given temperature at zero pressure, K'_{0T} is its first derivative in relation to the pressure and K''_{0T} is its second derivative in relation to the pressure.

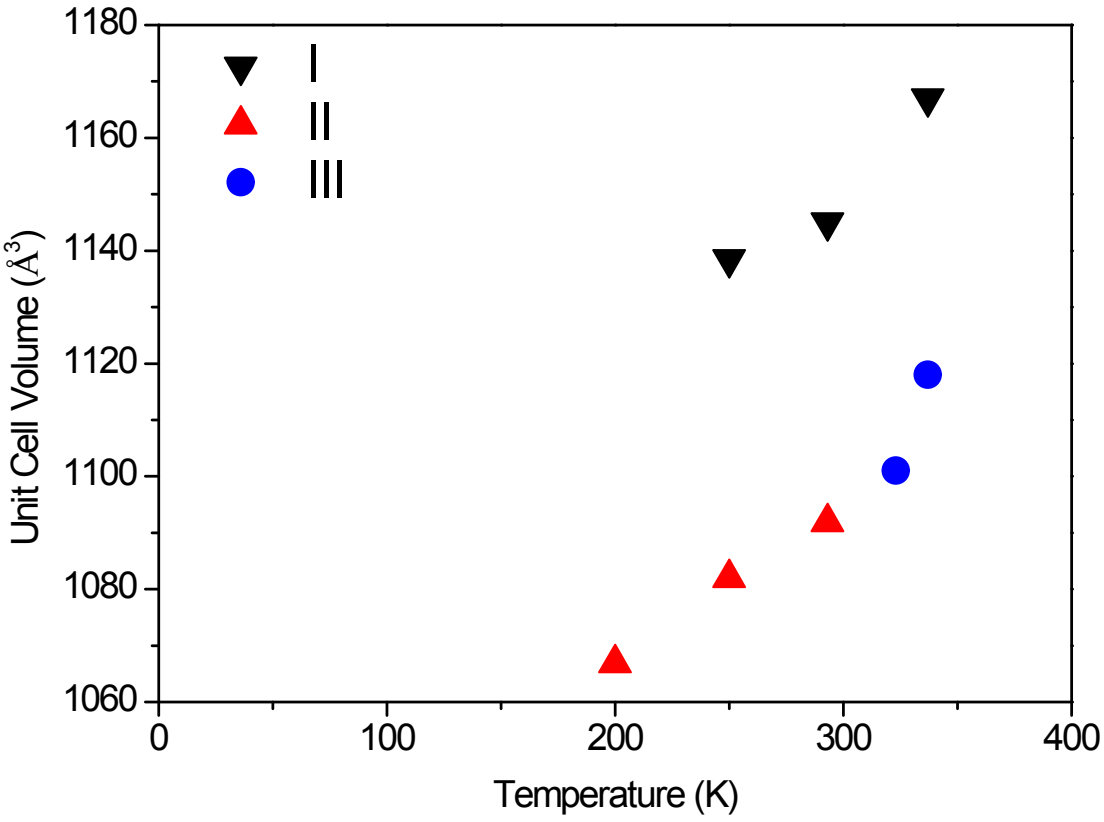

Figure S7. Unit-cell volume at zero pressure (V_{0T}) for polymorphs I (black inverted triangles), II (red triangles), and III (blue circles) obtained by fitting the Birch-Murnaghan equation to the $P(V)$ data in the paper

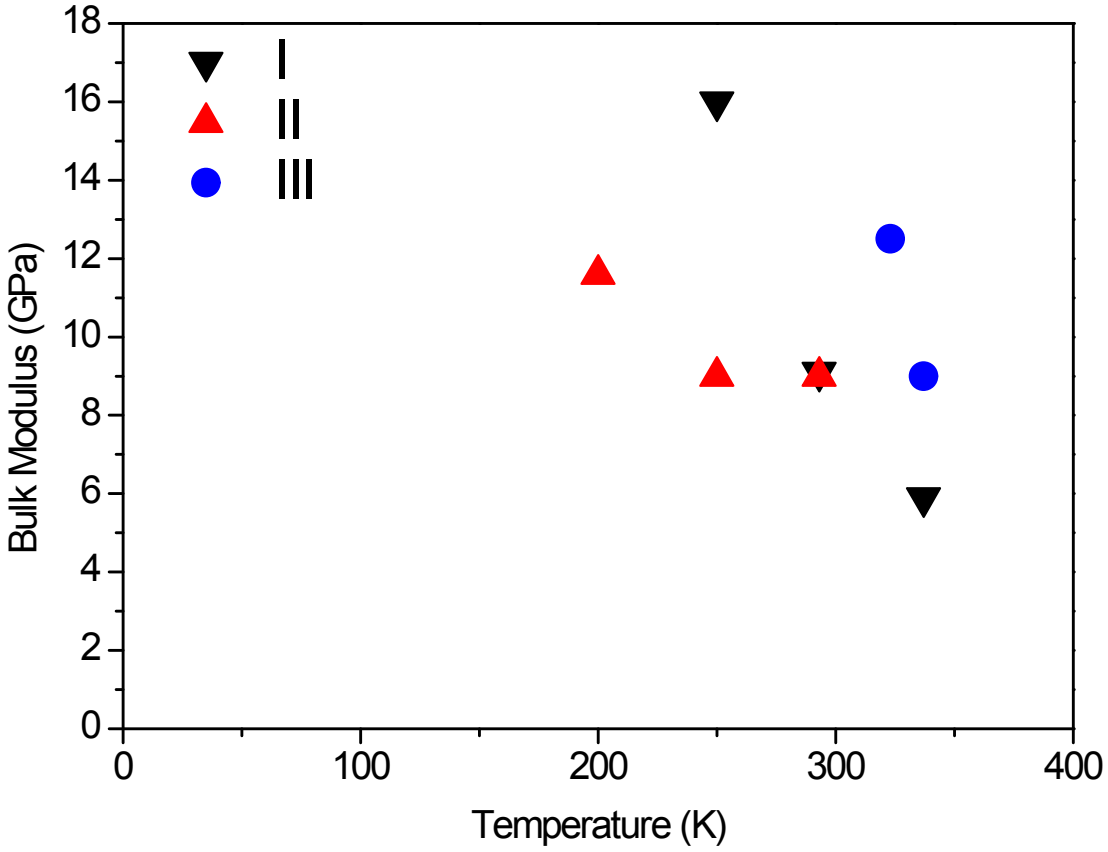

Figure S8. Bulk-modulus at zero pressure (K_{0T}) for polymorphs I (black inverted triangles), II (red triangles), and III (blue circles) obtained by fitting the Birch-Murnaghan equation to the P(V) data in the paper

References:

1. Nicolaï, B.; Mahé, N.; Céolin, R.; Rietveld, I. B.; Barrio, M.; Tamarit, J.-L., Tyrosine alkyl esters as prodrug: the structure and intermolecular interactions of l-tyrosine methyl ester compared to l-tyrosine and its ethyl and n-butyl esters. *Struct. Chem.* **2011,** *22* (3), 649-659.

2. Rietveld, I. B.; Barrio, M.; Tamarit, J.-L.; Nicolaï, B.; Van de Streek, J.; Mahé, N.; Céolin, R.; Do, B., Dimorphism of the Prodrug L-Tyrosine Ethyl Ester: Pressure-Temperature State Diagram and Crystal Structure of Phase II. *J. Pharm. Sci.* **2011,** *100* (11), 4774-4782.

3. Nicolai, B.; Itié, J.-P.; Barrio, M.; Tamarit, J. L.; Rietveld, I. B., Thermodynamics by synchrotron X-ray Diffraction: Phase relationships and crystal structure of L-tyrosine ethyl ester form III. *CrystEngComm* **2015,** *17*, 3974-3984.